ELSEVIER

Journal of Nuclear Materials 266–269 (1999) 291–295

journal of nuclear materials

Heat flux distribution in the divertor-II of ASDEX Upgrade

A. Herrmann *, C.J. Fuchs, V. Rohde, M. Weinlich, ASDEX Upgrade Team

Max-Planck-Institut für Plasmaphysik, EURATOM Assoziation, 85748 Garching, Germany

Abstract

A new divertor was installed in ASDEX Upgrade and went into operation in spring of 1997. The divertor was designed to handle heat fluxes relevant to ITER-like scenarios. For this, the tiles expected to receive the maximum load (strike point modules) are hardened by the use of carbon fibre composites covering about 20% of the total divertor area. The maximum heat flux detected by thermography in a H-mode discharge is only 4 MW/m^2 or below for a total input power of 20 MW without radiating mantle, except some ELMs showing a moderately higher heat flux. A broad distribution of the power load found in the measured poloidal distribution of the heat flux as well as the energy distribution, shows that less than half of the power flowing into the divertor is received by the strike point modules. The remaining power is loaded to other tiles of the divertor, particularly the transition module and parts of the roof baffle near to the strike point modules. The reconstructed radiation pattern reveals that the fraction of power radiated outside the divertor is comparable for both geometries. But the radiated fraction inside the divertor is increased by 10–15% in the Lyra shaped divertor.

Keywords: ASDEX Upgrade; Heat flux; Divertor; Radiation loss

1. Introduction

The open divertor of ASDEX Upgrade (DIV-I) was replaced by a Lyra shaped divertor (DIV-II) designed to handle high heat fluxes expected for ITER like scenarios. The strike point modules of DIV-II were hardened by use of carbon fibre composites to withstand heat fluxes of up to 15 MW/m^2 for 2 s [1] These high heat fluxes were expected by extrapolating heat flux profiles measured in DIV-I to the DIV-II situation and taking into account the increased heating power of 25 MW coming into operation at ASDEX Upgrade in 1997.

A heating power of 20 MW for about 1 s was injected in several discharges and the heat flux and the energy deposition was monitored. First results, presented in this paper, show that the modified divertor can withstand such high heating powers.

2. Diagnostics

Together with the DIV-II a lot of diagnostics came into operation to monitor the divertor load and to characterize the radiation in the divertor region.

The target load is measured by 3 thermography systems (Fig. 1). The closed geometry of the Lyra shaped divertor allows no direct view to the outer strike point module from outside the divertor region. That's why a new thermography system had to be installed. The new system monitors the surface temperature via a 1.8 m long, 60 mm dia. relay optics and stainless-steel-mirrors mounted in the slits between the target tiles at one toroidal position. The older thermography system [2] is still used to measure the surface temperature of the retention and transition modules, as well as of the roof baffle. Both systems use an IR line camera with InSb detectors and a CAMAC based data acquisition system. The best time resolution is 130 μs/line, the spatial resolution is about 1.2 mm/pixel at the strike point modules and varies between 2 and 8 mm for the other divertor modules. The heat flux to the different components is routinely calculated using the 2D-Code THEODOR [2]. In addition to the fast line cameras a 2D IR camera

* Corresponding author. Tel.: +49 89 329901; e-mail: alh@ipp.mpg.de.

0022-3115/99/$ – see front matter
PII: S0022-3115(98)00531-5

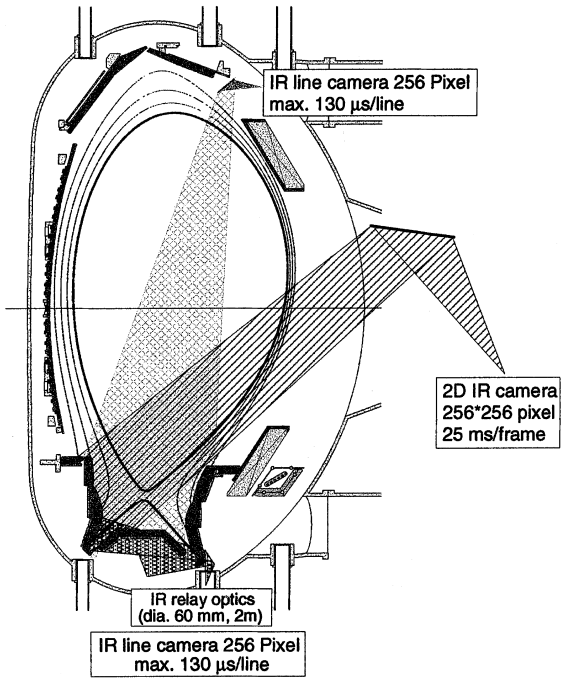

Fig. 1. Arrangement and field of view for the thermography systems used at ASDEX Upgrade.

measuring at video frequency was installed to monitor the toroidal and poloidal temperature pattern at one section of the inner divertor.

The line integrals of radiation losses are measured with a set of 22 divertor bolometers and 72 bolometers in the main chamber. The time resolution of the bolometer systems is 1 ms. The measured line integrals of radiation have been unfolded using the anisotropic diffusion model tomography [3] in order to reconstruct the radiation distribution in the divertor region as well as in the main chamber.

3. Experimental results

At ASDEX Upgrade plasma discharges with a wide parameter variation were performed. In this paper we focus mainly on H-mode discharges with high heating power (max. 20 MW NB heating) without impurity puffing, which should provide a critical test for the DIV-II performance.

An ELM averaged heat flux profile for a 20 MW NBI discharge is shown in Fig. 2. The spatial coordinate used is the distance along the divertor surface. The profile shown is a result of merging data from both line cameras. The measurements reveals a wide region with a moderate heat flux below 1 MW/m^2 and a heat flux peak

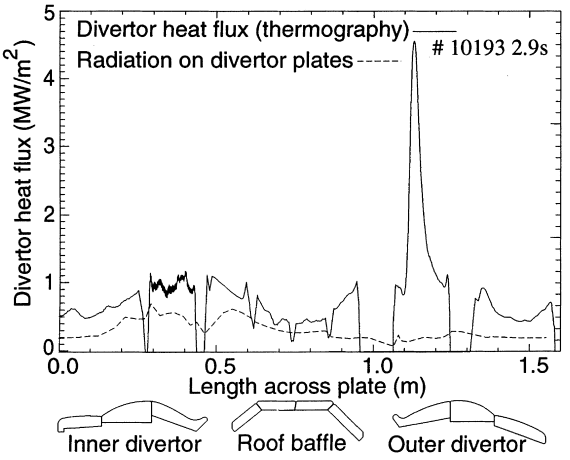

Fig. 2. Thermographical measured heat flux profile (solid line) and the heat flux to the divertor calculated from reconstructed radiation profiles (dashed line).

at the outer strike point. The maximum ELM averaged heat flux detected at the strike point module is below 5 MW/m^2. A significant heat flux peak could not be measured at the inner strike point module due to the titled arrangement shadowing the field of view in the inner divertor.

The 2D system was used occasionally to detect toroidal unsymmetries. The temperature distribution measured immediately after the end of a discharge represents the energy load to the divertor (Fig. 3). A 3D CAD view of the inner divertor is superimposed to the thermographic picture to make the view clear. The strike point modules are tilted to avoid edge heating. From the toroidal pitch angle and the target geometry follows, that about a quarter of each strike point module should be shadowed. The divertor is sensitive against mis-

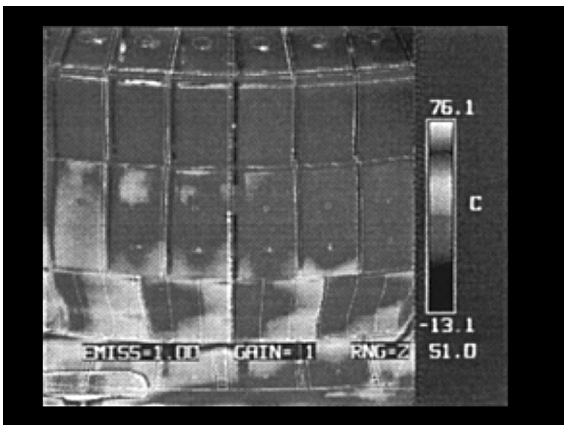

Fig. 3. Temperature pattern after the end of a NBI heated discharge (7 MW for 2 s, 4–8 × 10^{19} m^{-3}).

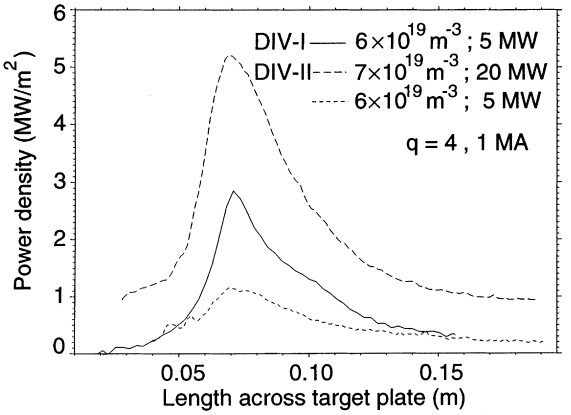

Fig. 4. ELM averaged heat flux profiles measured in divertor-I and II at the outer target plate.

alignment because of the sophisticated shape. The tilting and the misalignment causes the observed toroidal temperature variation across the other divertor components. Nevertheless, the strike point module is not heated essentially more than the transition module and the roof baffle.

In DIV-I as well as in DIV-II the maximum averaged heat load and the maximum energy load was detected at the outer divertor plate. Heat flux profiles across the outer target plates are compared in Fig. 4. The maximum heat flux in DIV-II is significantly reduced compared to DIV-I for the same global plasma parameters and input power. This reduction is not caused by simple geometrical reasons.

The conversion factor (inverse angle of incidence) to calculate the parallel heat flux at the outer plate shows Fig. 5 for both divertor configurations. Its radial variation across the divertor surface is much lower for DIV-II due to the fact that the shape of the DIV-II surface is matched to the field line configuration. However, the conversion factor is comparable for both geometries at the position of maximum heat flux. This means that the parallel power transported to the divertor plates is reduced in DIV-II. Up to now the characteristic parameters of the heat flux profiles are not investigated systematically, but the FWHM of DIV-II profiles are found to be broader compared to DIV-I profiles (Fig. 4).

For a set of H-mode discharges with heating energies up to 26 MJ/discharge, the energy accumulated by the divertor was calculated from thermography data by spatial and temporal integration. The fraction of energy accumulated by the different divertor parts is shown in Fig. 6(a). There is no energy dependence of the energy deposition found. The shot averaged distribution is given in Fig. 6(b), also indicating the individual divertor components.

The radiation pattern reconstructed from bolometric measurements allows to compare the radiation losses in different plasma regions for both divertor configurations. The radiation losses outside the divertor are comparable for DIV-I and DIV-II. 20% of the input

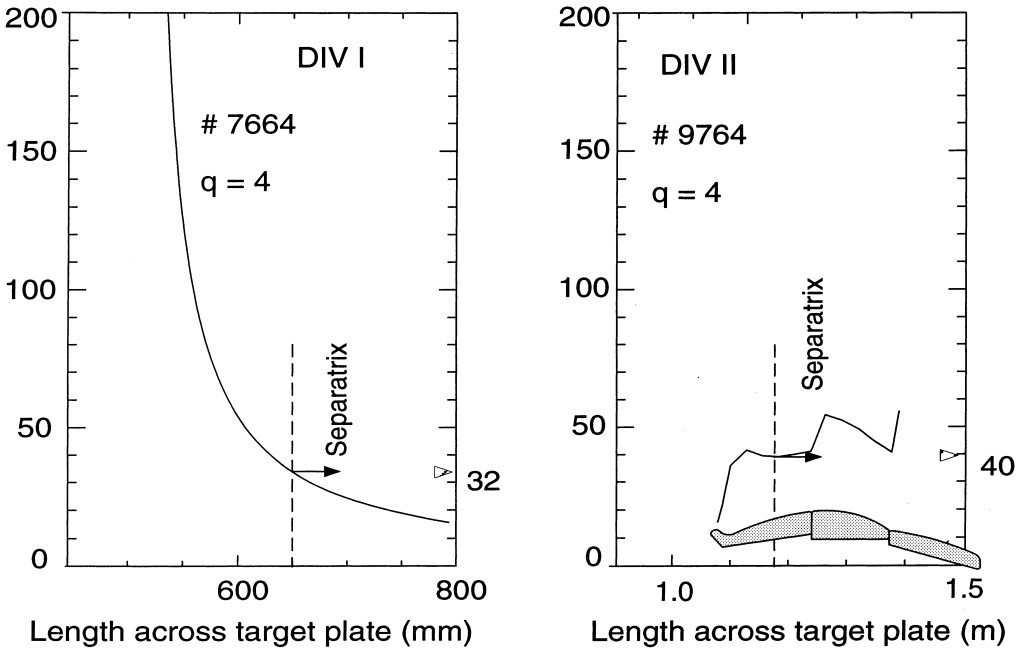

Fig. 5. Correction coefficient to calculate the parallel heat flux for both divertor geometries.

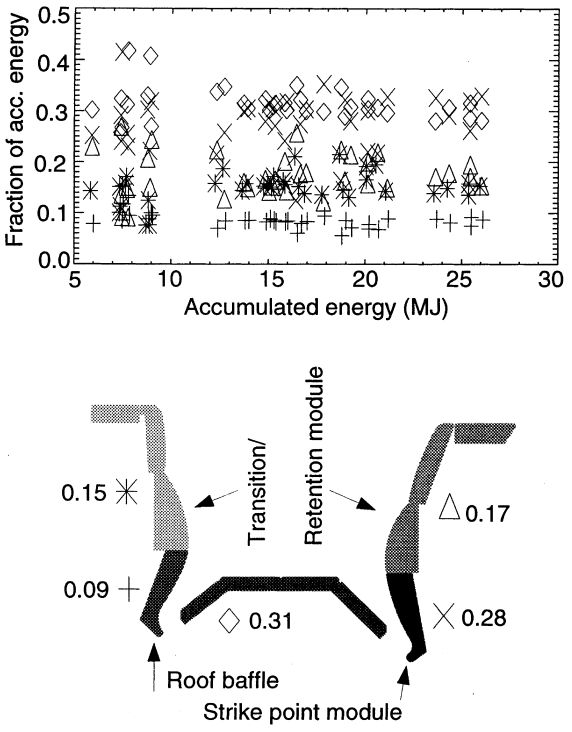

Fig. 6. (a) Energy accumulated by different divertor parts vs. shot accumulated energy [the meaning of the symbols is shown in (b)]; (b) shot averaged accumulated energy for main divertor sections.

power is radiated in the core 25–30% in the plasma edge and near the X-point. The remaining 45–50% of the input power has to dissipate in the divertor. In DIV-I 50–60% of the power flowing to the divertor is lost by radiation. This radiation loss is increased to about 70–80% in DIV-II. Due to this high fraction of radiation only 10–15% of the total input power is transported by heat conduction or convection to the divertor plates in DIV-II. The overwhelming fraction of radiated power in DIV-II is absorbed by the divertor structure due to the closed geometry. Radiation losses inside the divertor are measured both by bolometry and thermography.

The reconstructed radiation pattern are used to calculate the resulting heat flux to the divertor surface. It reveals, that except for the outer strike point module, most of the heat flux measured by thermography is caused by radiation (Fig. 2). Fig. 7 shows a power balance for a high power shot taking into account the contribution of radiation heating in DIV-II.

4. Discussion

Measurements of the divertor heat flux and radiation show that the Lyra shaped divertor of ASDEX Upgrade

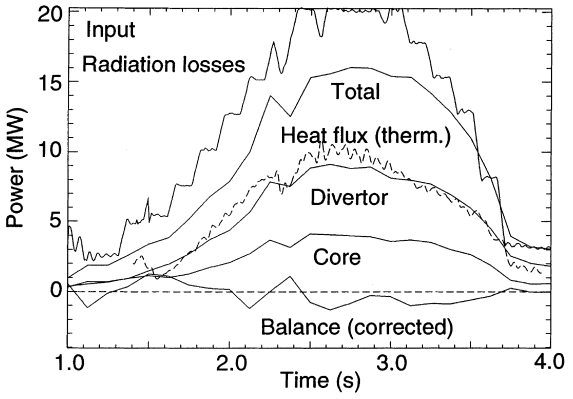

Fig. 7. Power balance for a 20 MW discharge showing the input power, the total radiation losses, divertor radiation, divertor heat flux measured by thermography, core radiation and the balance (corrected by the radiation contribution to the thermographical measured heat flux).

allows an input power of 20 MW without reaching a critical value for divertor heat flux or energy accumulation.

From thermographic and bolometric measurements, it follows that though the fraction of input power transported to the divertor region is the same for DIV-I and DIV-II, the fraction of parallel transported power reaching the plates is reduced by a factor of about 3 (Fig. 4). This is caused by different detachment properties for both divertor configurations. Whereas DIV-I is an open divertor DIV-II was optimized for neutral losses near to the separatrix region. The mechanism proposed for the power loss in the divertor region is a consequence of the low electron temperature even in the attached case in the outer divertor leg. Larger radial energy transport predicted by code calculations enhance the radiating volume [4]. Due to the low electron temperatures the energy transport becomes convective and feeds a broader radial zone compared to conductive heat transport. A detailed discussion of the power loss mechanism in the divertor region is given in [5]. The contribution of carbon release is discussed in [6].

The benefit of increased radiation loss is the broad distribution of the heat flux resulting in a heat flux level below 1 MW/m^2 for divertor components. The peak heat load of 5 MW/m^2 at 20 MW input power found at the outer strike point module is again below the critical value of 15 MW/m^2 assumed for the design of DIV-II [1]. Extrapolating the maximum heat flux to ITER using P/R, 39 and 5 MW/m, respectively, results in 13 MW/m^2 which is slightly higher the critical value of 10 MW/m^2 allowed for ITER. It should be mentioned that the peak heat flux during a type-I ELM exceeds the ELM averaged value by a factor of 2–3 (ASDEX Upgrade) up to a factor of 100 (JET) de-

pending on the ELM duration and the model of heat flux calculation [7].

Fig. 6 reveals that about 30% of the divertor load is accumulated by the outer strike point module. This amount is also expected from the power balance and the assumption that the energy not radiated is transported to the outer strike point. Another 30% of divertor energy is accumulated by the roof baffle due to the larger area compared to the retention/transition modules and the vicinity to the radiating regions. The heat load to the inner strike point region is negligible.

Extrapolating the energy load and the maximum surface temperature measured a discharge length of 10 s with 20 MW heating power should be tolerable for DIV-II of ASDEX Upgrade.

5. Conclusion

Although the energy reaching the divertor region is about the same for both divertor configurations the heat flux is spread over a wider region in DIV-II. The Lyra shaped divertor configuration increases the radiation losses inside the divertor region to 40–50% of the input power. This level is about 15% higher compared to DIV-I, resulting in a reduced maximum heat flux. The maximum ELM averaged heat flux is about 5 MW/m^2 also for an input power of 20 MW ($P/R = 15$ MW/m).

References

[1] IPP-Report IPP 1/281.
[2] A. Herrmann, W. Junker, K. Günther et al., Plasma Phys. Control. Fusion 37 (1995) 17.
[3] J.C. Fuchs, K.F. Mast, A. Herrmann et al., Contrib. 21st EPS (1994) 1308.
[4] S. Krasheninikov et al., Contrib. Plasma Phys. 36 (1996) 266.
[5] R. Schneider, H.-S. Bosch, D. Coster et al., these Proceedings.
[6] A. Kallenbach, A. Baard, D. Coster et al., these Proceedings.
[7] S. Clement, A. Chankin, D. Ciric et al., these Proceedings.